wooden sarcophagus from the treasures of King Tutankhamon, which bore the inscription of Queen Tiye. In 1975, the Michigan expedition reopened the side chamber of the tomb of Amenhotep II to secure a sample of the hair of the "Elder Lady" and the following week obtained a hair sample from the locket of Queen Tiye in the Egyptian Museum.

In the summer of 1976, a series of control hair samples along with mummy hair samples were analyzed. They were subjected at cross section to ion etching and scanning electron microprobe analysis. The correlation of data allowed the identification of dispersive x-ray energy for the various elements present in each sample. The results of this information when recorded in a memory control center allowed for the recall and comparison of many samples on a cathode-ray tube. The results show a near perfect superimposition of two samples on a graphic display tube (Fig. 5). These results strongly support the argument that the hair samples from both King Tutankhamon's tomb and the mummy from Amenhotep II's tomb are indeed those of the same person—Queen Tiye of the Eighteenth Dynasty, wife of Amenhotep III and mother of the heretic pharaoh Amenhotep IV or Akhenaton.

JAMES E. HARRIS
School of Dentistry, University of Michigan, Ann Arbor 48109
EDWARD F. WENTE
Department of Egyptology, Oriental Institute, University of Chicago, Chicago, Illinois 60637
CHARLES F. COX
School of Dentistry, University of Michigan
IBRAHIM EL NAWAWAY
Egyptian Museum, Cairo
CHARLES J. KOWALSKI
School of Dentistry, University of Michigan
ARTHUR T. STOREY
School of Dentistry, University of Manitoba, Winnipeg R3E 0W3, Canada
WILLIAM R. RUSSELL
Department of Radiology, Medical School, University of Michigan
PAUL V. PONITZ
GEOFFREY F. WALKER
School of Dentistry, University of Michigan

References and Notes

1. G. Elliot Smith, *The Royal Mummies, Catalogue Général des Antiquities du Egyptiennes du Musée du Cairo, Nos. 61051-61100* (Service des Antiquities de l'Egypte, Cairo, 1912), p. 1.
2. J. E. Harris and K. R. Weeks, *X-raying the Pharaohs* (Scribner, New York, 1973), p. 93.
3. W. M. Krogman, in *An X-ray Atlas of the Royal Mummies*, J. E. Harris, Ed., in preparation.
4. G. F. Walker and C. J. Kowalski, *Growth* 35, 191 (1971).
5. M. R. Anderberg, *Cluster Analysis for Applications* (Academic Press, New York, 1973), p. 1.
6. We thank Drs. Moukhtar, H. Riad, A. K. Salem, A. B. El Sadre, L. Aboul-Ela, S. Aboul Azam, R. Saad, M. El-Soghier, G. Walker, Z. Iskander, and W. M. Krogman and M. Abdul Mohsen and S. Abdelal. Supported by NIH PL480 research agreement 03-011-N (formerly 5X2511), National Institute of Dental Research grant 5 R01-DE 03013-10, the Smithsonian Institution, Michigan Memorial Phoenix Project, Biomedical Research Resources, the Public Health Service, and the Eastman Kodak Corporation.

1 November 1977; revised 15 February 1978

Visualization and Transport of Positron Emission from Proton Activation in vivo

Abstract. *Heavy charged particle beams can be widely used for cancer therapy if control in heterogeneous tissue is proved practical. A beam of protons at 200 million electron volts has been visualized in plastic and in a living animal by using an on-line positron camera. The fraction of the activity retained in the radiation site was found to be at least 70 percent of that produced in a dead animal. The sensitivity of the technique was established for a typical geometry.*

The application of heavy charged particles (pions, protons, alpha particles, and heavier ions) in radiation therapy is prompted by the potential improvement they offer in dose distribution compared to neutral radiation (*1*). Differences in radiobiological properties of some of these particles may also be useful. Energetic beams of heavy charged particles are penetrating enough to irradiate deep-seated tumors. The depth of the peak dose and of the maximum beam penetration is dependent on beam energy and tissue composition, particularly inhomogeneities of density in the beam path (*2*). General therapy with these beams requires control of the beam distribution in heterogeneous tissue; and of particular importance is the surface of maximum beam penetration. If the end of the beam path is used to spare normal tissues just beyond the tumor, failure to compensate accurately for density variations in the beam path may result in overdose to those normal tissues or underdose to part of the tumor.

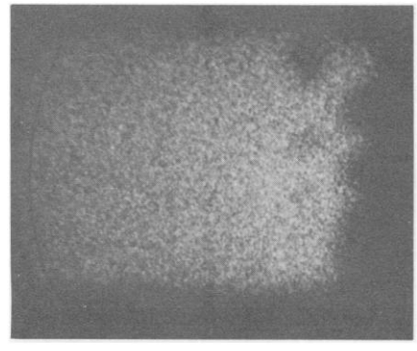

Fig. 1. Scintigram of positron emission activity induced in an acrylic plate by a proton beam. The acrylic was 4 cm thick, and holes with diameters of 1.9, 1.3, and 1.0 cm were bored through the plate at a depth of 17.8 cm from the beam entrance face (to the left of the camera field). Increased depth of penetration of the beam passing through the holes is clearly seen. Reduced activity within the holes can also be noted. The beam was 1 cm thick and 10 cm high; the dose was 22 rads. The initial beam energy was 190 MeV, corresponding to a maximum penetration of 23.7 g/cm² in acrylic. The threshold energy for positron activation is 20 MeV, corresponding to a residual range of 0.5 cm; thus the last 0.5 cm of beam penetration produces no activation. The event density is nearly constant along the beam path, but it appears to increase since the sensitivity is maximum at the center of the camera field, near the locus of maximum beam penetration.

One method for controlling heavy charged particle beams is visualization of the radioactivity generated by the beam in tissue. The primary radionuclides produced are ^{15}O (half-life, 2.05 minutes) and ^{11}C (half-life, 20.4 minutes). Both are positron emitters and are produced by nuclear interactions of beam particles with oxygen and carbon nuclei in tissue. Each positron interacts with an electron, producing a pair of 0.5-MeV gamma rays with nearly opposite directions. If the two gamma rays are detected in coincidence by two separate detectors, the positron-electron annihilation must have taken place somewhere along the straight line connecting the two detection sites.

This technique was suggested earlier for control of therapeutic beams of heavy charged particles (*3*). Previous studies were limited to physical measurements (*4*), calculations (*5*), and off-line localization of long-lived activation products, particularly ^{11}C (*6*). Further development has been hampered by the requirement of a suitable, dedicated imaging device, the danger of activation of the detector itself, and questions of the mobility of the radionuclides generated.

We report here preliminary results of studies of the distribution of positrons generated by a 200-MeV proton beam and detected by an on-line positron cam-

0036-8075/78/0609-1151$00.50/0

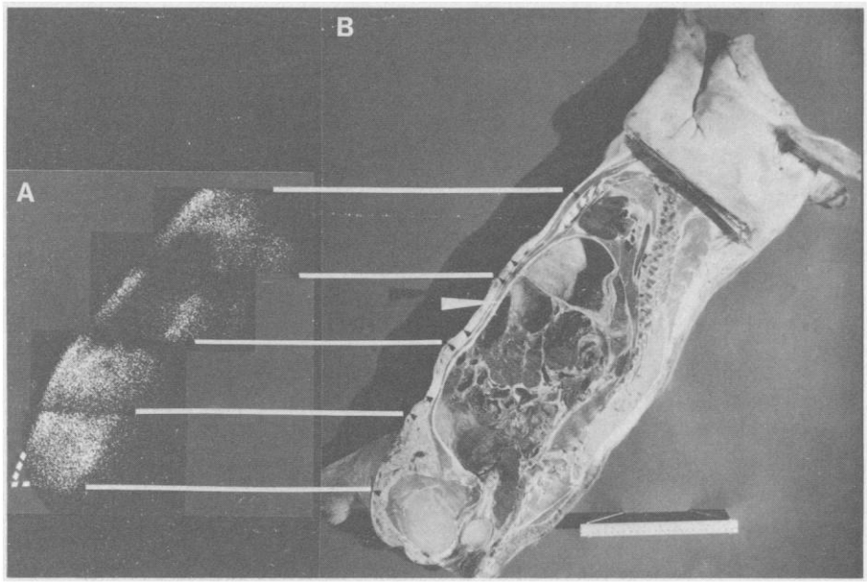

Fig. 2. (A) Montage of positron scintigrams of a live pig. Each of the four scintigrams was generated by a proton beam 15 cm high and 1 cm thick; there is a 3-cm overlap on adjacent fields. The beam was incident on the ventral surface, on the sagittal plane. The peak dose for each field was 22 to 29 rads. An acrylic absorber 9 g/cm² thick was inserted in the beam path to reduce maximum beam penetration to 14 cm of muscle tissue. Note that the positron camera field of view cuts off events near the ventral surface in the bottom field. (B) Cross section of the dead pig along the beam plane. The animal was frozen in the same attitude used in irradiation to maintain its internal geometry. The small black wedges near the ventral surface indicate the entrance locations of the four overlapping beams that produced the scintigrams shown in (A). The large white wedge indicates the center of second field and the beam direction. Scale bar, 25 cm.

era. The maximum depth of proton beam penetration in water or muscle was 23 cm. The beam was 1 cm wide to limit activity to the focal plane of the positron camera. The positron camera consists of two position-sensitive detectors, used to register the positions of impact of pairs of coincident gamma rays that emerge from the test object. The detectors are 39 cm in diameter and are parallel to and 36 cm each from the beam plane.

Figure 1 is a positron scintigram showing the proton-induced activity in a thick acrylic plate with holes 1.9, 1.3, and 1.0 cm in diameter. The end-of-range contour of the beam after traversing the 1-cm hole is clearly resolved. The limiting resolution of the positron camera, determined from tests with a point source, is less than 9 mm (full width at half-maximum).

The activity generated in vivo in a pig is shown in Fig. 2A, a montage of positron scintigrams taken after four irradiations of the animal along the sagittal plane. The contour of maximum penetration after traversal of bone, lung, muscle, and air can be seen in all but one field. In the second field the maximum depth contour was displaced beyond the positron camera field of view by the unexpected void in the upper abdomen. This void was confirmed in the anatomical section after the animal was killed and frozen (Fig. 2B) and in lateral radiographs taken sequentially with the scintigrams.

The sensitivity with the present apparatus is greater than seven detected events per gram of interacting tissue on the camera axis, per rad of peak dose. Ultimately, the sensitivity will be increased by a factor of 3 by increasing the thickness of the detector crystals from 1.27 to 2.54 cm, and by another factor of 3 by decreasing the detector separation to 40 cm. Further increases in the sensitivity would be gained at some sacrifice in spatial resolution. No significant activation of the detectors has been observed, partly because of factors related to beam and collimator design.

For therapy the treatment volume can be sampled "slice by slice," and an absorber shaped to bring the beam end to the desired locus. The dose required is about 10 percent of the therapeutic dose per treatment. After each treatment the activity induced by the beam can be recorded and used for computer reconstruction of the three-dimensional dose distribution throughout the treatment volume. This offers a mechanism for quality control of the therapeutic process, which is presently unavailable.

Transport of activity from the generation site is to be expected from diffusion and circulation. On-line detection permits analysis of this phenomenon. In preliminary studies of the biological transport of radionuclides induced in rat muscle, we compared the activity in locally irradiated volumes in live and dead animals. Least-squares analysis of the decay curves resolved the components ^{15}O, ^{11}C, and (in smaller amounts) ^{13}N in both states, but only live animals exhibited a component with a half-life of 2/3 minute, which was ascribed to biological transport and which accounted for less than 20 percent of the total activity generated. A similar result was obtained with the pig (Fig. 2). A comparison of positron events detected in the upper field of Fig. 2A, produced by irradiations before and after the animal was killed, showed 29 percent fewer events within the field in the live animal. The activity transported from the generation site appears to be diluted into a large volume, producing a very small background. Measurement of the spatial resolution in living rats revealed no discernible change compared to that in dead animals.

Studies of biological transport of radionuclides generated in vivo should provide information that will be useful in localizing and reconstructing the dose of therapeutic beams of ions and pions. In addition, refinements of the technique should permit the study of regional blood flow following activation in vivo.

G. W. BENNETT
Department of Nuclear Energy, Brookhaven National Laboratory, Upton, New York 11973
J. O. ARCHAMBEAU
Department of Radiation Oncology, City of Hope Medical Center, Duarte, California 91010
B. E. ARCHAMBEAU
University of Chicago, Chicago, Illinois 60637
J. I. MELTZER
Department of Radiation Oncology, Nassau County Medical Center, East Meadow, New York 11554
C. L. WINGATE
Department of Radiology, School of Medicine, State University of New York, Stony Brook 11790

References and Notes

1. This was proposed by R. R. Wilson more than 30 years ago [*Radiology* **47**, 487 (1947)]. The total dose to normal tissues was calculated to be two to five times less with a proton beam than with gamma rays [J. O. Archambeau, J. W. Bennett, G. S. Levine, R. Cowen, A. Akanuna, *ibid.* **110**, 445 (1974)]. Comparable but smaller reduction factors are anticipated for negative pions and heavy ions.
2. In bone, muscle, and air the beam loses energy

at a rate approximately proportional to the density of the material traversed. Beam penetration is shallower in bone than in muscle; in air and air-filled tissue penetration is increased by an amount about equal to the length of the air path traversed.

3. Attributed to C. A. Tobias in (*6*).
4. M. C. Taylor, G. C. Phillips, R. C. Young, *Science* **169**, 377 (1970).
5. G. W. Bennett and J. O. Archambeau, *Nucl. Instrum. Methods* **125**, 333 (1975).
6. H. D. Maccabee, U. Madhvarath, M. R. Raju, *Phys. Med. Biol.* **14**, 212 (1969).
7. Supported by grant CA-188347 from The National Institutes of Health and by contract EY-76-C-02-0016 with the Department of Energy.

5 December 1977; revised 28 February 1978

Acute Myelogenous Leukemia: A Human Cell Line Responsive to Colony-Stimulating Activity

Abstract. *A permanent human cell line that maintains the granulocytic characteristics of acute myelogenous leukemia cells has been established. The cells of this line form myeloid colonies in soft gel culture in the presence of human colony-stimulating activity. The cell line may be useful for studying human acute myelogenous leukemia and the mechanism of response to colony-stimulating activity.*

Research on acute myelogenous leukemia in humans has been impeded by the lack of an adequate model system. Leukemia in rodents does not parallel the human disease, and continuous cell lines from patients with acute myelogenous leukemia usually lose their myeloid characteristics in vitro (*1*).

We describe here a cell line (KG-1) which was derived from a 59-year-old man with erythroleukemia that developed into acute myelogenous leukemia. This cell line retains its granulocytic nature in vitro and forms myeloid colonies in soft gel culture in response to colony-stimulating activity (CSA). The patient's bone marrow contained 30 percent myeloblasts and 10 percent erythroblasts with marked megaloblastic and dysplastic changes. The patient died of sepsis 2 months after study. Cells obtained by bone marrow aspiration were placed in T flasks with alpha medium (Flow) containing 20 percent fetal calf serum, penicillin, streptomycin, and $10^{-4}M$ α-thioglycerol; the cultures were incubated at 37°C in an atmosphere of 5 percent CO_2 in air. After 24 days in culture, the cells were actively proliferating. They have since been passaged 52 times in an 8-month period. The cells grow in suspension and do not form clumps. Whenever the cells were transferred in the liquid culture, there was an initial 1-day lag phase followed by growth with a mean doubling time of 70 to 80 hours, until cell densities of 2.5×10^6 to 3.5×10^6 cells per milliliter were reached.

The cultured cells morphologically resemble acute myelogenous leukemia cells, with 98 percent myeloblasts and promyelocytes, 2 percent intermediate and late stage granulocytes, and rare macrophages (Fig. 1). More than 85 percent of the cells stain positively for naphthol AS-D chloroacetate esterase (Sigma); 98 percent stain positively for acid phosphatase; 52 percent give a positive reaction with periodic acid–Schiff reagent; 10 percent are peroxidase positive; and a rare macrophage-like cell has a positive reaction with α-naphthyl butyrase (Fig. 1). These cytochemical characteristics are typical of moderately well-differentiated acute myelogenous leukemia. Medium from 5-day cultures that had been initiated with 3×10^6 cells contained lysoenzymes at 5.5 ± 1.2 μg/ml.

Chromosomal abnormalities were consistently observed upon cytogenetic examination with standard methodology and banding technique (*2*). Metaphase studies of 19 consecutive cells showed 45 chromosomes, and banding of five cells showed 45,XY,(5p$^+$9q$^-$),−12,−17, +MAR,+fragment. Epstein-Barr virus (EBV) nuclear antigen and the EBV capsid antigen were not present. The leukemic cells had HLA-A30 and HLA-B35 histocompatibility antigens, assayed by microcytotoxicity (*3*). A human granulocyte-specific antigen was detected by microcytotoxicity on KG-1 cells by 8 of 40 human granulocyte-reactive antiserums (*4*). A B lymphocyte–associated or Ia-like antigen was detected on 20 percent of the cultured cells (*5*). This antigen was previously found in leukemic cells from 70 percent of patients with acute myelogenous leukemia (*5*).

Surface membrane immunoglobulin was not demonstrable by immunofluorescence. No rosette formation occurred with sheep erythrocytes, but 7 ± 3 percent of the cells formed rosettes with antibody-coated sheep red blood cells. The cells did not respond to phytohemagglutinin (PHA) by an increase in [^{3}H]thymidine incorporation. The cultured cells used had a minimal (3 percent) ability to lyse chromium-labeled murine lymphoblasts (EL-4) by antibody-dependent cell-mediated cytotoxicity (*6*). The cultured leukemic cells did not phagocytose opsonized *Candida albicans* (*7*), but 29 ± 5 percent ingested one or more 1-μm latex particles. The

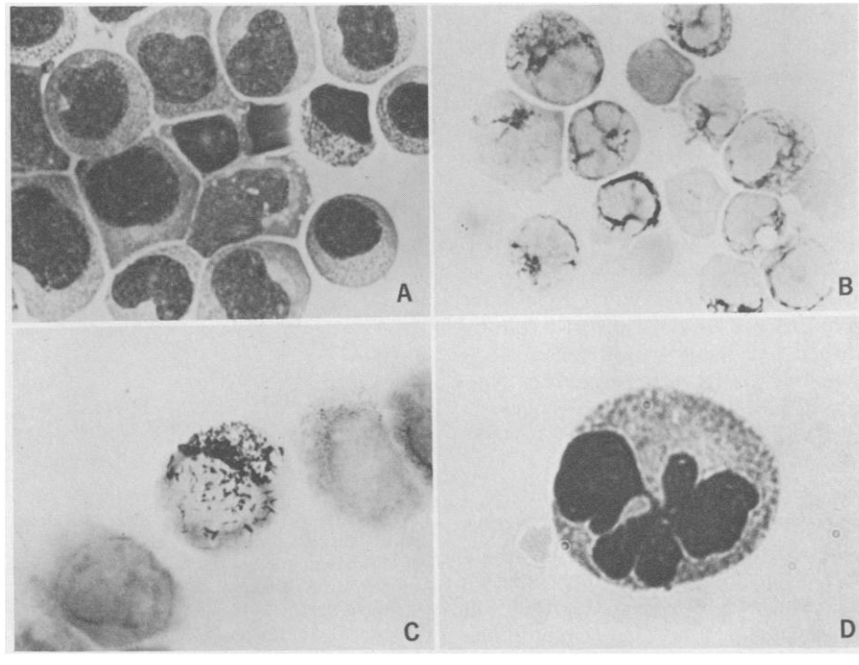

Fig. 1. Morphological characteristics of KG-1 cells in liquid culture. (A) Early and intermediate stage granulocytes stained with Giemsa (×400). (B) Numerous naphthol AS-D chloroacetate esterase-positive cells (×256). (C) Prominent peroxidase-positive cell (×400). (D) Multilobed polymorphonuclear granulocyte (×640).

0036-8075/78/0609-1153$00.50/0